Cryogenics 49 (2009) 669–671

Contents lists available at ScienceDirect

Cryogenics

journal homepage: www.elsevier.com/locate/cryogenics

SQUID current amplifiers for sub-kelvin operation temperatures

J. Pleikies [a,*], O. Usenko [b], G. Frossati [b], J. Flokstra [a]

[a] Low Temperature Division, Faculty of Science and Technology, University of Twente, P.O. Box 217, 7500 AE Enschede, The Netherlands
[b] Kamerlingh Onnes Laboratory, Leiden University, P.O. Box 9504, 2300 RA Leiden, The Netherlands

ARTICLE INFO

Article history:
Received 17 July 2008
Received in revised form 25 November 2008
Accepted 27 December 2008

Keywords:
F. SQUID systems
C. Thermoacoustics
C. Heat transfer
A. Thin films
D. Temperature sensors

ABSTRACT

Extremely sensitive current sensors are being developed by integrating input coils on superconducting quantum interference devices (SQUIDs) and optimizing them for being cooled to the mK temperature range. The most important effects for this type of sensors are investigated in this paper. SQUID characteristics were experimentally studied at mK temperatures and in numerical simulations, revealing a crucial hysteretic effect originating from parasitic elements introduced by the integrated coil. Furthermore, the cooling behavior of shunt resistors with attached cooling fins, dominated by the hot-electron effect, was investigated. A numerical model allows to reproduce the experimental data in a good way.

1. Introduction

Low-Tc dc-SQUIDs are being developed for utilization in the gravitational wave antenna MiniGRAIL [1]. A low-noise operation of the SQUID amplifier with the resonant load requires a minimum reachable additive and back-action noise at the target temperature of 20 mK and at frequencies in the kHz-range. The intended input inductance in the μH range should have a good coupling efficiency and thus has to be integrated on the SQUID chip. The results from our first designs, which were fabricated at the IPHT Jena [2], gave insights into mainly two areas that will be sketched in the following two sections: issues related to the SQUID dynamics and the cooling behavior of the sensors, dominated by the hot-electron effect.

2. SQUID dynamics

The performance of SQUID sensors with integrated input coils can be heavily influenced by parasitic capacitances. Comparable sensors have already been under investigation for a long time, as can be seen in e.g. [3–6]. Still it is no trivial task to predict the behavior of the fabricated device during the design process.

Two designs were made, a dc-SQUID with integrated flux-transformer and a dc-SQUID with a highly symmetric layout separating the feedback and the signal coil systems [7]. The sensors showed unexpected behavior by means of partly distorted and hysteretic characteristics, originating from parasitic elements introduced by the integrated input coils. Nevertheless, a good noise of 155 fA/$\sqrt{\text{Hz}}$ referred to the current through the coupling coil was reached for one SQUID at bath temperatures below 300 mK [7]. This corresponds to a calculated energy resolution of 60 ħ referred to the SQUID loop.

To be able to understand the behavior of the SQUIDs from Ref. [7] and to predict and optimize the performance of future developments, we concentrated on numerical simulations on realistic models of SQUIDs including the radio frequency interaction of the coil and the washer structure [6]. We were able to reproduce the measured characteristics and sensitivity in a good way [8]. As shown in Fig. 1, we observed a hysteresis originating from resonances in the washer structures in the numerical simulations as well as in an experimental re-investigation of the phenomenon. The hysteresis is caused by the coil resonance [6], where the wavelength roughly corresponds to the double of the length of the coupling coil. For the SQUID shown in Fig. 1, the coil resonance of the 60 integrated windings occurs at a corresponding voltage $f{\cdot}\Phi_0$ of about 0.1 μV [8]. When the SQUID is switching from the superconducting state to the voltage state, it starts to oscillate with a frequency higher than the named resonance frequency. The effective SQUID inductance can dramatically change during this transition [6]. Speaking in terms of the standard theory [9] the SQUID is switching to a lower β_L-value and is forced to a working point with a higher voltage and oscillation frequency. In case of the SQUID shown in Fig. 1, β_L is decreasing from about 1.8 in the superconducting to 1.1 in the voltage state. This hysteresis has only been explicitly observed in numerical simulations before [3–5].

The optimum operation frequency of a dc-SQUID, which has to be predicted during the design process, is typically given by the following numerically achieved equation, see e.g. [9]:

* Corresponding author. Tel.: +31 53 4893125; fax: +31 53 4891099.
E-mail address: j.pleikies@tnw.utwente.nl (J. Pleikies).

0011-2275/$ - see front matter
doi:10.1016/j.cryogenics.2008.12.020

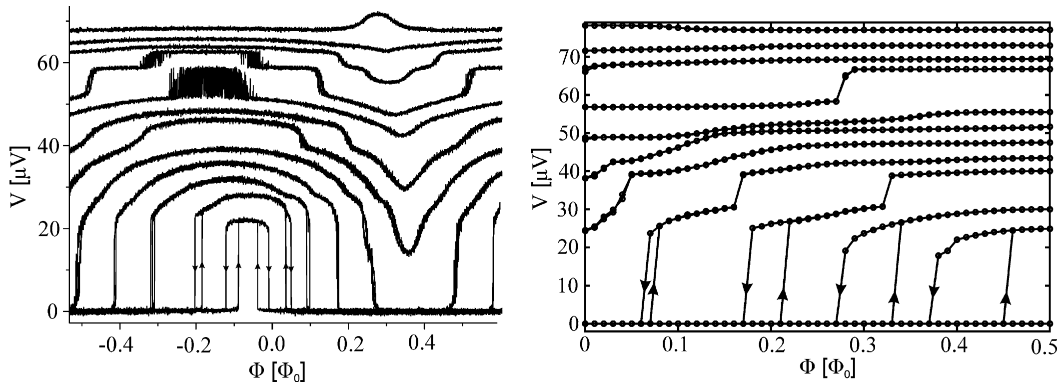

Fig. 1. Measured (left) and simulated (right) flux vs. voltage characteristics of the dc-SQUID with integrated flux-transformer at a bath temperature of 0.1 K and different bias currents. The figure was taken from Ref. [8]. The effective temperature in the measurement is, depending on the working point, increased – see the section on the thermal behavior. Hysteretic paths are indicated by arrows. In the figure on the left a single flux sweep was measured back and forth for each bias current. Applied bias currents are from 17 (bottom) to 35 μA (top) for the measurement on the left and 12 (bottom) to 36 μA (top) for the simulation on the right.

$$f_{OP} \approx 0.3 I_0 R / \Phi_0 \tag{1}$$

Here, I_0 is the critical current of a Josephson junction, R is the shunt resistance and Φ_0 is the magnetic flux quantum 2.07×10^{-15} Wb. In a sensor comparable to ours, a low-noise operation in the in Eq. (1) given working range can easily be ruled out by the hysteresis originating from this coil resonance, even if its resonance frequency is orders of magnitude below f_{OP}. One is forced to operate the SQUID at higher voltages, most suitable still far away from other typical resonance points [6]. Therefore, the target working point has to be chosen carefully including the hysteresis and other direct resonance effects.

3. Thermal behavior

Another important issue we investigated is the thermal behavior of the sensing device. The sensitivity of practical dc-SQUIDs cooled down to temperatures below 1 K is typically limited by the hot-electron effect [10]. Here an increased thermal resistance due to a weakened electron–phonon coupling leads to a higher temperature of the electrons in the thin film shunt resistors, as described by the following equation [10]:

$$P = \sum \Omega (T^5 - T_b^5) \tag{2}$$

Here, P is the dissipated power, Σ is a material dependent constant, Ω is the volume of the resistor, T is the effective temperature of the electrons and T_b is the bath temperature which is assumed to be equal to the phonon temperature. Thus the power dissipated in a SQUID sensor is limiting the electron temperature in its shunt resistors and their Johnson noise. This leads to a saturation of the noise of SQUID sensors cooled to extremely low temperatures [10].

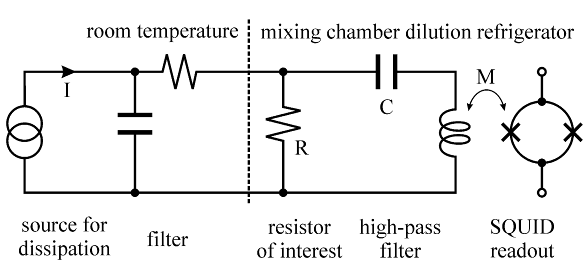

Fig. 2. Schematic of the setup to measure the electron temperature in resistors. The temperature of the electrons is determined from the Johnson noise, measured by a SQUID. The high-pass filter allows a controlled dissipation via a dc current source situated at room temperature. The low temperature part was placed in a dilution refrigerator to reach the bath temperatures of interest, down to about 50 mK.

We included test structures with resistors of the typical geometrical size and resistance value of the shunt resistors attached to our SQUIDs on the same wafer as the SQUID sensors described above. The *PdAu* resistors are contacted by superconducting pads. By dissipating power and measuring the Johnson noise of the resistor via a SQUID, we could determine the effective electron temperature. The corresponding measurement setup is shown in Fig. 2. We found a good agreement with Eq. (2), a fit of the measurement data at different bath temperatures and power dissipation allowed us to determine the material constant Σ of *PdAu* to 0.79×10^9 W K^{-5} m^{-3}, using the volume of the shunt resistor of 15·42·0.11 μm^3.

Cooling fins (CFs), electrically negligible extensions of the volume of the resistor, can be attached to improve the cooling behavior by providing a reservoir of cold electrons that exchange with the hot-electrons in the volume of heat dissipation [10]. The thermal behavior of such a system is besides the hot-electron effect determined by the heat conduction via the electrons within the geometry of resistor and cooling fin, as described by the following partial differential equation [11]:

$$P/A = \sum d(T^5 - T_b^5) - \nabla (L d \rho^{-1} T \nabla T) \tag{3}$$

Here the most left term is only active in the area A of dissipation, the area of the resistor. d is the film thickness, L is the Lorentz number 2.45×10^{-8} W Ω K^{-2}, ρ is the specific resistivity and ∇ is the Nabla operator.

We also performed measurements on resistors of the same dimensions as the one described above but with attached cooling fins in a *Au* layer of 100 nm thickness of differing size and shape. A sample measurement of one structure at different bath temperatures is shown in Fig. 3.

Eq. (3) was numerically solved in two dimensions by the finite elements method (FEM) and the result for the different bath temperatures are shown by solid lines in Fig. 3. The determined value Σ for *PdAu* was used here, the Σ of 2.4×10^9 W K^{-5} m^{-3} for *Au* was taken from literature [11,12]. d and ρ for the *Au* and *PdAu* layers were taken from the design values [2]. A similarly good agreement was found for all three characterized resistors with differing cooling fins.

In Fig. 4 a FEM-based comparison of the different configurations is shown at the same bath temperature. This calculations and of course also the measurement data show that the cooling fins help to reduce the electron temperature at lower ranges of power dissipation, but unfortunately their effect vanishes for a dissipation comparable to the one in the shunt resistors of our SQUIDs in the

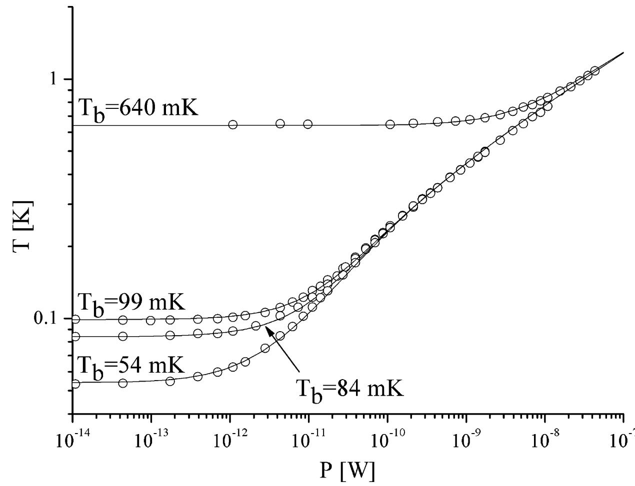

Fig. 3. Measured (circles) and calculated (solid lines) electron temperature vs. power characteristics for a resistor with attached cooling fin of 80·280 μm². The calculations are FEM-based solutions of Eq. (3), as described in the text.

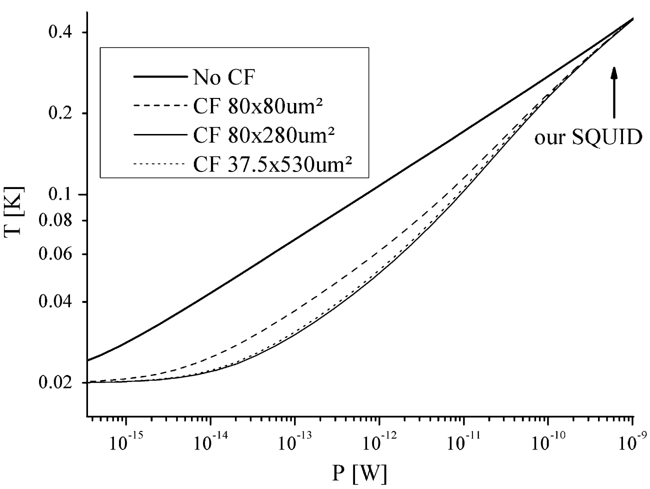

Fig. 4. FEM-based comparison of the characterized configurations of resistors without a CF and with CFs of differing geometry. The bath temperature was set to 20 mK. The arrow indicates the power dissipation in a shunt resistor of our SQUID sensor of about 0.6 nW.

order of a nanowatt. The main measures for improving the cooling behavior of future SQUIDs are on the one hand to use materials with a larger hot-electron material constant Σ and a lower resistivity ρ and on the other hand to increase the volume of the shunt resistor itself to both reduce its stand-alone electron temperature and to improve the effect of a connected cooling fin [10,11,13].

4. Conclusions

We gained insights into mainly two areas influencing the performance of SQUID-based current sensors. On the side of the SQUID dynamics, we observed a hysteresis that has to be taken into account while optimizing a wide range of SQUID sensors with many-turns integrated input coils. A careful modeling and numerical simulations appear to be the best way to include this effect.

Furthermore, the performed measurements and numerical calculations on the hot-electron effect gave insights into the thermal budget of the sensors. Due to the hot-electron effect, the electron system in the shunt resistors is easily pushed out of thermal equilibrium with the phonon system. The measurements and the numerical model showed that attached cooling fins only help to reduce the effective temperature at low power dissipation. A main measure for improving the cooling behavior is to increase the volume of the resistor to a maximum. This is again restricted by the dynamics of the SQUID and the Josephson junction to damp due to parasitic inductances and capacitances introduced by the shunt resistor. Accordingly, this also requires a good electromagnetic modeling and preferable numerical simulations.

References

[1] De Waard A, Gottardi L, Van Houwelingen J, Shumack A, Frossati G. MiniGRAIL, the first spherical detector. Class Quantum Grav 2003;20(10):143–51.
[2] LTS SQUID process at IPHT Jena. Institute of Photonic Technology e.V., POB 100239, D-07702 Jena, Germany. Technology details from correspondance and from design-rules, online at <http://www.ipht-jena.de/photonic-instrumentation/departments/quantum-detection/technologiesfoundry.html> (July 2008).
[3] Ryhänen T, Seppä H, Cantor R. Effect of parasitic capacitance and inductance on the dynamics and noise of dc superconducting quantum interference devices. J Appl Phys 1992;71(12):6150–66.
[4] Drung D, Jutzi W. Hysteretic noise simulation of dc SQUIDs with input coil. In: Hahlbohm HD, Luebbig H, editors. SQUID '85. Berlin, New York: Walter de Gruyter; 1985. p. 807–12.
[5] Tesche CD. Analysis of a double-loop dc SQUID. J Low Temp Phys 1982;47(5):385–410.
[6] Enpuku K, Cantor R, Koch H. Modeling the direct current superconducting quantum interference device coupled to the multiturn input coil. II. J Appl Phys 1992;71:2338.
[7] Pleikies J, Usenko O, Kuit KH, Flokstra J, De Waard A, Frossati G. SQUID developments for the gravitational wave antenna MiniGRAIL. IEEE Trans Appl Supercond 2007;17(2):764–7.
[8] Pleikies J, Usenko O, Flokstra J. Numerical studies on dc-SQUID sensors with tightly coupled input coil. J Phys Conf Ser 2008;97:012254.
[9] Clarke J, Braginski AI. The SQUID Handbook, vol. I. Weinheim: Wiley-VCH; 2004.
[10] Wellstood FC, Urbina C, Clarke J. Hot-electron effects in metals. Phys Rev B 1994;49(9):5942–55.
[11] Giazotto F, Heikkilä TT, Luukanen A, Savin AM, Pekola JP. Opportunities for mesoscopics in thermometry and refrigeration: Physics and applications. Rev Mod Phys 2006;78:217.
[12] Echternach PM, Thoman MR, Gould CM, Bozler HM. Electron–phonon scattering rates in disordered metallic films below 1 K. Phys Rev B 1992;46(16):10339–44.
[13] Savin AM, Pekola JP, Averin DV, Semenov VK. Thermal budget of superconducting digital circuits at subkelvin temperatures. J Appl Phys 2006;99:084501.